Academic Sciences International Journal of Pharmacy and Pharmaceutical Sciences

ISSN- 0975-1491 Vol 5, Suppl 4, 2013

Research Article

EFFECTS OF A LIPOPHILIC ISONIAZID DERIVATIVE ON THE GROWTH AND CELLULAR MORPHOGENESIS OF *MYCOBACTERIUM TUBERCULOSIS* H37Rv

THAIGARAJAN PARUMASIVAM[1*], HAWALA SHIVASHEKAREGOWDA NAVEEN KUMAR[1], SURIYATI MOHAMAD[2], PAZILAH IBRAHIM[1], AMIRIN SADIKUN[1]

[1]School of Pharmaceutical Sciences, Universiti Sains Malaysia, Penang, Malaysia, [2]School of Biological Sciences, Universiti Sains Malaysia, Penang, Malaysia. Email: perak_thaiga@yahoo.com.

Received: 21 Jan 2013, Revised and Accepted: 11 Sep 2013

ABSTRACT

Objectives: We analyzed the effects of a chemically synthesized hydrophobic isoniazid (INH) derivative, 1-isonicotinoyl-2-hexadecanoyl hydrazine (INH-C16) at its minimum inhibitory concentration (MIC) on *Mycobacterium tuberculosis* H37Rv with respect to cell viability, cellular morphology, and acid-fastness properties. The observations were compared to that of INH.

Methods: The effects of INH and INH-C16 at concentration of 0.0781 µg/mL and 0.0391 µg/mL respectively on the growth characteristics and cellular morphology of *M. tuberculosis* H37Rv were studied using colony count assay, light microscopy (LM), scanning electron microscopy (SEM) and transmission electron microscopy (TEM).

Results: INH-C16 exhibited similar strength of cidal effects as INH on the mycobacterial cells, even though the MIC value of INH-C16 was lower than INH. Observations under LM indicated that the INH and INH-C16 affected the growth and cellular morphology as well as the acid-fastness properties of the treated cells. Subsequent electron microscopic observations revealed the rupture in the envelope of the treated cells resulting in the extrusion of cellular materials. This caused the cells to shrink and eventually die.

Conclusion: Increasing the hydrophobicity of INH by augmentation of hydrophobic side chain would enhance the anti-TB activity of the drug. It could also be assumed that the added hydrophobic side chain in INH-C16 metabolized in such a way that liberated the active form of INH inside the mycobacteria and inhibited the mycolic acid synthesis.

Keywords: 1-isonicotinoyl-2-hexadecanoyl hydrazine; Acid-fastness properties; Anti-tuberculosis; Isoniazid.

INTRODUCTION

It is undeniable that isoniazid (INH) is a transcendent first-line anti-tuberculosis (TB) drug in TB therapy regimen. INH is also known as isonicotinic acid hydrazide and isonicotinyl hydrazine. The primary target of INH is the inhibition of mycolic acid synthesis[1, 2]. Mycolic acid is a long-chain α-alkyl-β-hydroxy fatty acid; a major component in the cell wall of *Mycobacterium tuberculosis*[3]. This component plays a vital role in maintaining the integrity of the mycobacterial cell wall[4]. Therefore, the suppression of mycolic acid biosynthesis leads to cellular malformation and eventual cell death.

However, the burgeoning incidence of INH resistant *M. tuberculosis* strains in the last decades has complicated the TB treatment[5, 6]. Several INH resistant mechanisms against *M. tuberculosis* have been proposed. These include mutations in the gene encoded for INH activator peroxidase (*katG*), enoyl acyl carrier protein (ACP) reductase (*InhA*), b-ketoacyl ACP synthase (*kasA*), alkyl-hydroperoxide reductase (*ahpC*), NADH dehydrogenase (*ndh*), and also inactivation of INH by *nat*-encoded arylamine *N*-acetyltransferase[3, 7-12]. Other studies suggested that the architecture of the cell envelope also contributes to *M. tuberculosis* resistance, whereby, the outer layer of the cell wall hinders the diffusion of chemotherapeutic agents into the cell, thus, causing resistance by exclusion barrier[13-16].

Interestingly, numerous studies have suggested that the anti-mycobacterial activity of INH could be enhanced against *M. tuberculosis* as well as *M. avium* complex by augmenting the hydrophilic INH with a hydrophobic/lipophilic side chain[14-17]. Based on these antecedents, a lipophilic INH-derivative, 1-isonicotinoyl-2-hexadecanoyl hydrazine (INH-C16) was chemically synthesized by augmenting the side chain of INH with 16 carbon acyl chain. Hence, in this study, we examined the effects of INH-C16 on the growth and cellular morphology of *M. tuberculosis* H37Rv.

MATERIALS AND METHODS

Organism

A 10-day old *M. tuberculosis* H37Rv ATCC 25618 culture grown on Middlebrook 7H10 agar (Difco, USA) enriched with 0.5 % glycerol and 10 % oleic acid-albumin-dextrose-catalase (OADC) at 37 ˚C in 8 % CO_2 was used throughout this study.

Isoniazid derivative

The INH-C16 was chemically synthesized following the procedure outlined by Besra et al.,[18]. Dry dichloromethane and 4-dimethylaminopyridine (1.2 eq.) were added to the hexadecanoyl chloride, followed by INH (Sigma-Aldrich, UK) (1.1 eq.). The reaction mixture was stirred at ambient temperature overnight and then washed with 2% dilute hydrochloric acid and water. The organic layer was dried over anhydrous magnesium sulphate. The solvent was removed under reduced pressure to obtain the crude product which was purified by column chromatography. Product confirmation was achieved by standard procedures involving IR, ^{1}H-NMR, ^{13}C-NMR, mass spectroscopy, and CHN analysis. Stock solutions of INH and INH-C16 (1 mg/mL) were prepared by dissolving the compounds in distilled water and dimethyl sulfoxide (DMSO) respectively. These stock solutions were further diluted in distilled water to attain the desired working concentrations. These working solutions were then filter-sterilized prior to usage.

Minimum Inhibitory Concentration (MIC) determination

The MIC values of INH and INH-C16 were determined using tetrazolium microplate assay (TEMA) following the procedures by Caviedes et al.,[19]. MIC determination using TEMA method is less laborious, cheaper, and much faster, compared to the conventional proportion method which requires a very long incubation period of 3-4 weeks. The experiment was conducted in a sterile 96-well microplate in triplicates twice. Initially, the outer wells were added with 200 µL of sterile distilled water followed by Middlebrook 7H9 broth into wells in columns 3 until 11 in rows 2 to 6. A volume of 100 µL of drug solution was added in triplicates into wells in columns 2 and 3, and then serially diluted from columns 3 to 4 until 10. The last 100 µL of the solution was discarded. A volume of 100 µL of log phase bacterial suspension at a dilution of 1.5 x 10^7 CFU/mL was added into all test wells. The wells in column 11 functioned as negative controls (without drugs). The plates were sealed and incubated at 37 °C in 8 % CO_2 for 5 days. On the 5th day,

50 µL of Tetrazolium-Tween 80 mixture (Tetrazolium [3-(4,5-dimethylthiazol-2-yl)-2,5diphenyl-tetrazolium bromide] with concentration of 1 mg/mL in absolute ethanol and 10 % Tween 80 at 1:1) was added into one control well and incubated for 24 hours. If the control well turned from yellow to purple, tetrazolium-Tween 80 mixture was added to all wells and incubated for another 24 hours. If well B11 remained yellow, incubation was continued and the tetrazolium-tween 80 mixture added to wells C11, D11, E11, F11, and G11 on day 7, 9, 11, 13, and 15 respectively. The MIC was defined as the lowest drug concentration that prevented conversion of tetrazolium dye from yellow to purple.

Studies on effects of INH-C16 on growth and cellular morphology of *M. tuberculosis* H37Rv

A volume of 2 mL McFarland no. 3 mycobacterial inoculum was transferred into three separate bottles containing 18 mL of Middlebrook 7H9 broth. The first bottle served as a control. The second bottle contained INH at its MIC value of 0.0781 µg/mL. The third bottle contained INH-16 at its MIC value of 0.0391 µg/mL. The bottles were then incubated at 37 °C in 8 % CO_2 for 12 days. Samples were taken daily for the colony counts using Miles and Misra drop plate method[20]. Tenfold serial dilutions (10^{-2}, 10^{-3}, 10^{-4}, and 10^{-5}) of the culture samples were prepared in phosphate buffer saline (PBS) solution. A volume of 20 µL of each diluent was dropped in triplicates onto two sets of Middlebrook 7H10 agar plates. The plates were then allowed to dry at room temperature, sealed and incubated at 37 °C in 8 % CO_2 for 21 days. After incubation, the colonies were counted and CFU/mL was calculated.

Simultaneously, 100 µL of the mycobacterial inoculum was spread onto three sets of seven Middlebrook 7H10 agar plates in duplicates. The first set served as a control without addition of drugs. The second set contained INH at a final concentration of 0.0781 µg/mL and the third set contained INH-C16 at a final concentration of 0.0391 µg/mL. The plates were then incubated at 37°C in 8 % CO_2 for 12 days. The cell samples were harvested selectively on day 0, 1, 2, 4, 6, 8, 10, and 12 for the microscopic observations of the cellular morphology and acid-fastness properties.

Observation of cellular morphology and acid-fastness properties under light microscope (LM)

The Ziehl-Neelson (hot) acid fast procedure was performed using TB Stain Kit ZN (BD, USA) prior to examination under the LM. The smears were examined microscopically with oil immersion objective to observe the cells using Olympus BX51 bright field microscope (OLYMPUS DP72) equipped with a digital camera and connected to a computer. In this study, the cells that retained acid-fastness properties were stained bright red. The faintly coloured cells were referred to as "ghost" cells.

Electron microscopy observations

The pellet was prepared from the bacterial cells collected from respective test plates as explained earlier and suspended in PBS (pH 7.2). The cells were then centrifuged at 5000 rpm for 5 minutes. The supernatant was discarded and the pellet was resuspended in *McDowell-Trump* fixative solution prepared in 0.1 M PBS for at least 2 hours. The cells were then washed with 0.1 M PBS and post-fixed in osmium tetraoxide prepared in PBS and followed by twice post-fix washings with distilled water. For the observation under scanning electron microscope (SEM), a portion of the pellet was then put through a dehydration process through a series of 50 %, 75 %, 95 %, and 100% ethanol followed by hexamethyldisilazane (HMDS). The HMDS was decanted and left in a desiccator to air-dry at room temperature. The dried cells were mounted onto a SEM specimen tub with a double-sided sticky tape and coated with gold. The cells were then observed under Leo Supra 50VP Field Emission SEM equipped with Oxford INCA 400 energy dispersive x-ray microanalysis system (Carl-Ziess, Germany). For the observation under transmission electron microscope (TEM), the other portion of the bacterial pellet was mixed with 2 % agar solution and cut into small blocks (approximately 1 mm^3). These agar cubes were dehydrated through a series of 50 %, 75 %, 95 %, and 100% ethanol and finally with 100 % acetone. Samples were then embedded in Spurr resin and cut into ultrathin sections using ultramicrotome. The ultrathin sections were mounted on copper grids, stained with uranyl acetate and lead citrate, washed with distilled water and viewed under EFTEM LIBRA 120 equipped with an Olympus sis-iTEM (Carl-Ziess, Germany).

RESULTS

Minimum inhibitory concentration determination

The chemical structures of INH and INH-C16 are shown in Fig. 1. The MIC of INH and INH-C16 were 0.0781 µg/mL and 0.0391 µg/mL respectively. Further studies on the effects of INH-C16 and INH on the viability and cellular morphologies of *M. tuberculosis* were carried out at these respective MIC values.

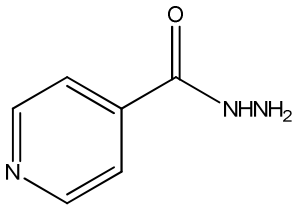

(a) Isoniazid

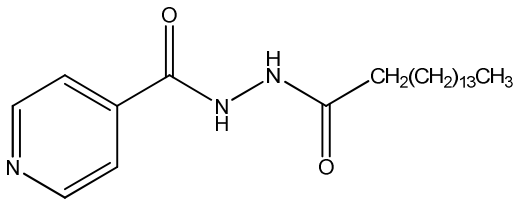

(b)1-isonicotinoyl-2-hexadecanoyl hydrazine

Fig. 1: The chemical structures. (a) isoniazid (INH) and (b) 1-isonicotinoyl-2-hexadecanoyl hydrazine (INH-C16).

Effects of INH-C16 on the growth of *M. tuberculosis* H37Rv

Fig. 2 illustrates the results obtained. The control culture displayed a normal growth curve with a sharp increase in the colony counts in the first 24 hours which gradually stabilized until day 10 and then, followed by a slow decrease until day 12. In general, the cells treated with INH and INH-C16 exhibited almost similar patterns of growth. In these cultures, there was a steady decrease of colony counts throughout the 12 days. By the end of the study period only about 25% of the initial cell population remained viable.

Cellular morphological studies under light microscope (LM)

In general, the cellular morphological changes were very difficult to assess in detail under LM observation due to the small size of the mycobacterial cells. Hence, in this report, we highlight only the obvious changes with regards to cell shapes, sizes and staining properties. The cell types were described as: rods or bacilli of 2.0 ± 0.44 µm in length (Fig. 3 arrow A); coccobacilli (Fig. 3 arrow B); elongated bacilli of 3.1 ± 1.09 µm in length (Fig. 3 arrow C); amorphous clumps (Fig. 3 arrow D); and "ghost cells" (Fig. 3 arrow E).

The control culture, on day 0 consisted of a few rods. After 24 hours, most of the cells were observed as elongated bacilli. By day 6, the cell population appeared heterogeneous consisting of rods and coccobacilli. From this day onward, the observation essentially remained the same for the rest of the experiment. With regard to acid-fastness, the cells retained their acid-fastness properties throughout the study period.

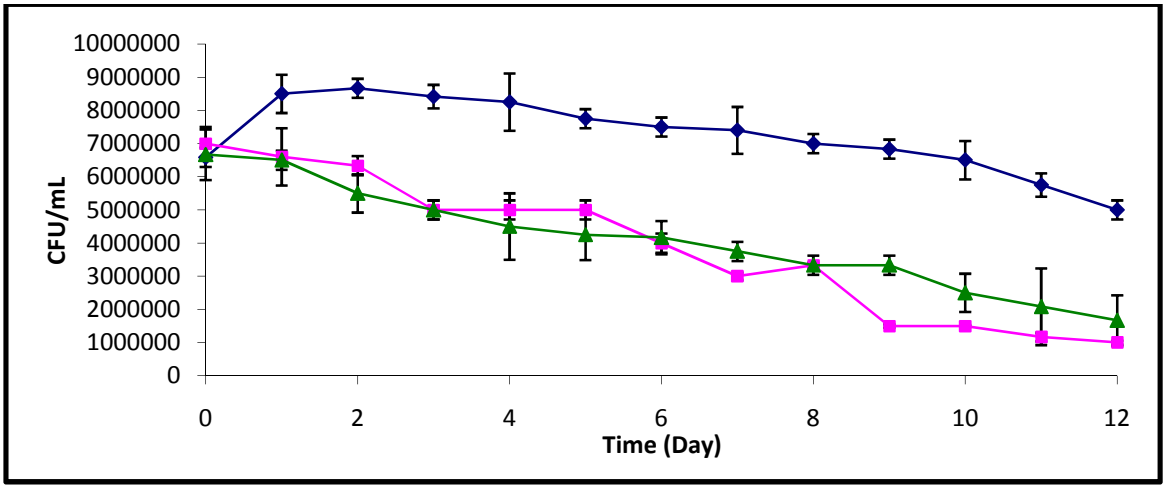

Fig. 2: Effects of isoniazid (INH) and 1-isonicotinoyl-2-hexadecanoyl hydrazine (INH-C16) on the colony counts of *Mycobacterium tuberculosis* H37Rv ATCC 25618. (♦) Control, (■ INH-treated, (▲) INH-C16-treated.

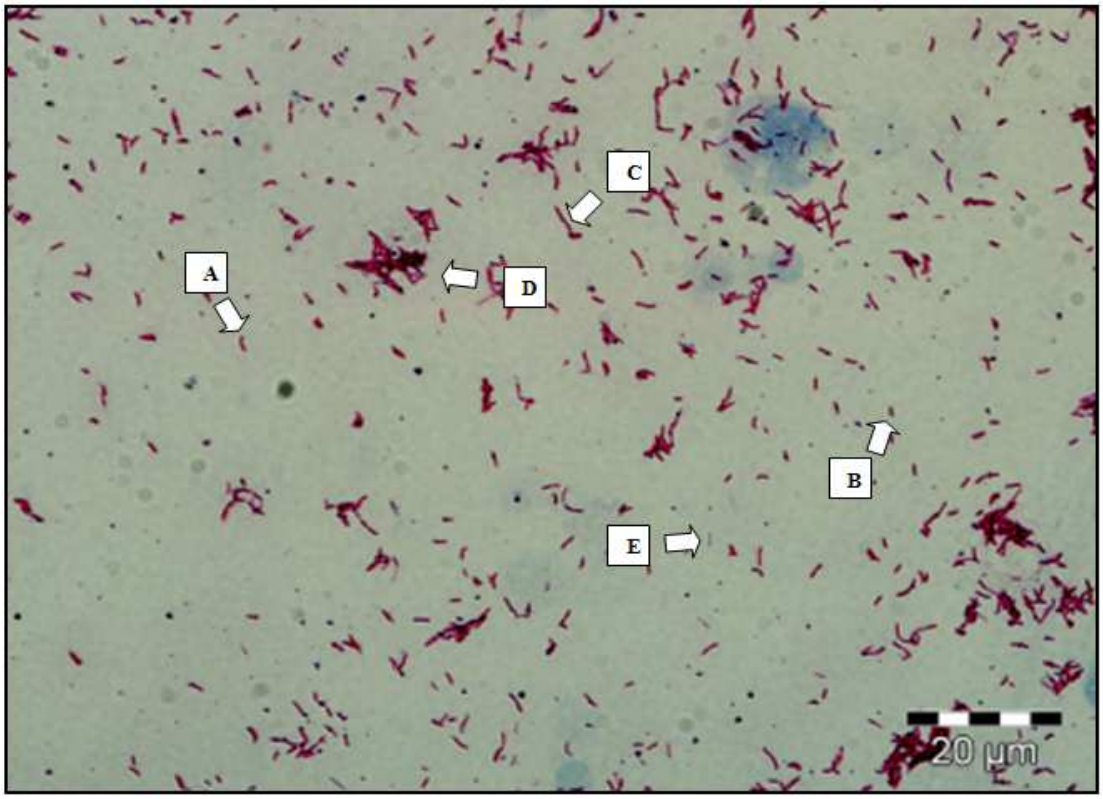

Fig. 3: Cellular morphology under light microscope. (A) small rods or bacilli, (B) coccobacilli, (C) elongated bacilli, (D) amorphous clumps, and (E) "ghost" cells.

The INH-C16-treated cells displayed almost similar morphological changes as the INH-treated cells. In summary, the cells in the drug-treated cultures were in a mixture of coccobacilli, rods, and elongated rods along with the presence of amorphous clumps. This resulted in the "messy" appearance of the cell population throughout the study period. The presence of "ghost" cells were also observed in an increasing number right from day 1 in these drug-treated cultures.

Observation under electron microscopes

Figure 4 (a) shows the *M. tuberculosis* cells in the control culture on day 2. The cells have a smooth surface with a well defined rigid rod shape. In addition, dividing cells were also observed which, are indicated by arrows A and B.

The cellular morphological effects of INH and INH-C16 treatments are presented by Figure 4 (b-h) and Figure 4 (i-o) respectively. The INH and INH-C16 exposed cells displayed almost similar morphological changes. After 24 hours of exposures, the cells appeared ragged and stuck to each other (Figure 4 (b-c) and (i-j)). Tiny holes were also observed on a few cells (indicated by arrows) with bulges at the ends. Figure 4 (d-e) and (k-l) shows a "web-like" material observed around the drug-treated cells on day 2 and day 4. By day 8, the cells appeared shrunk and the cell wall was ruptured leaving behind empty shells (Figure 4 (f) and (m)). Eventually, they formed an amorphous mass of cells (Figure 4 (g-h) and (n-o)).

Control

Day 2

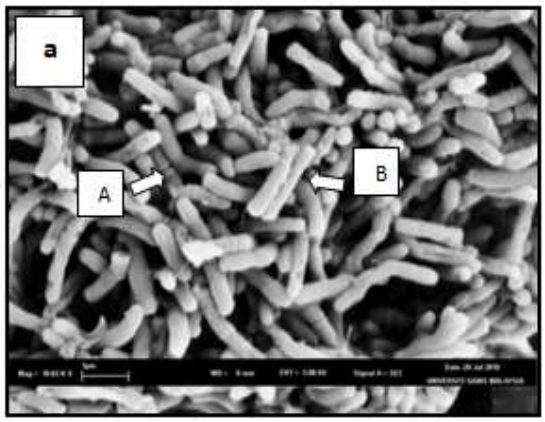

INH-treated cells **INH-C16-treated cells**

Day 1

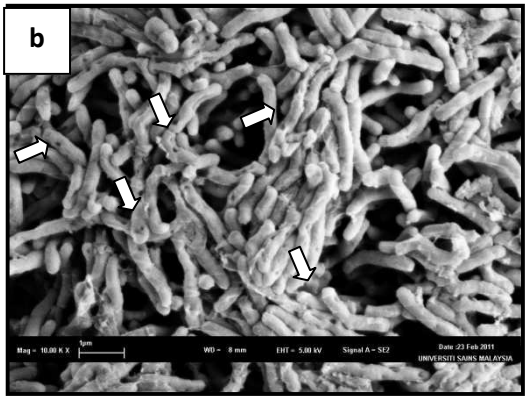

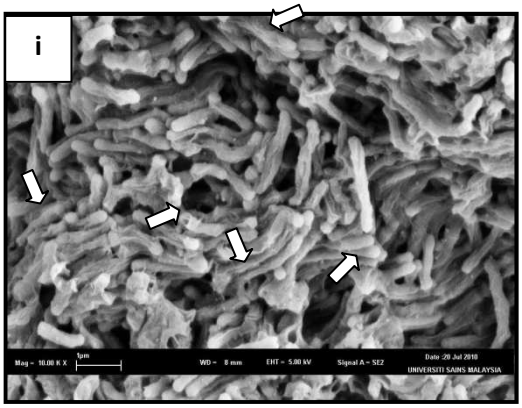

Day 2

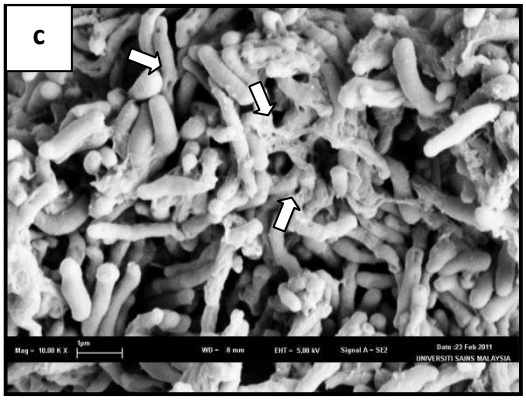

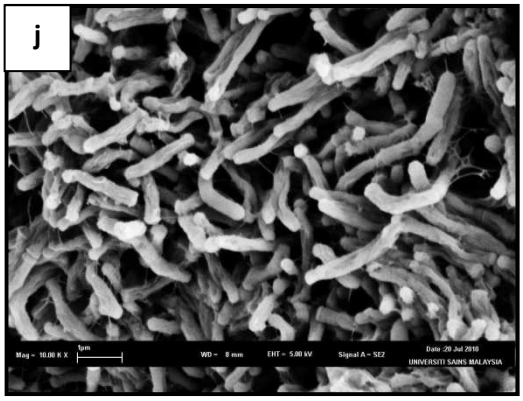

Day 4

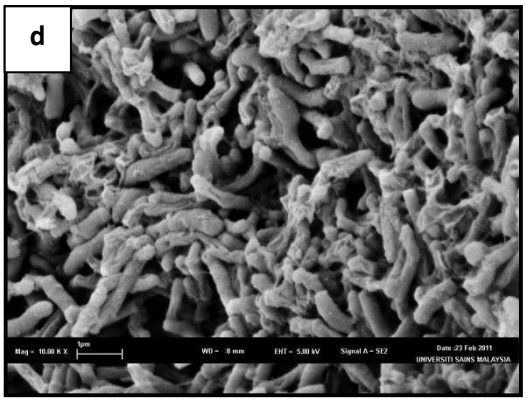

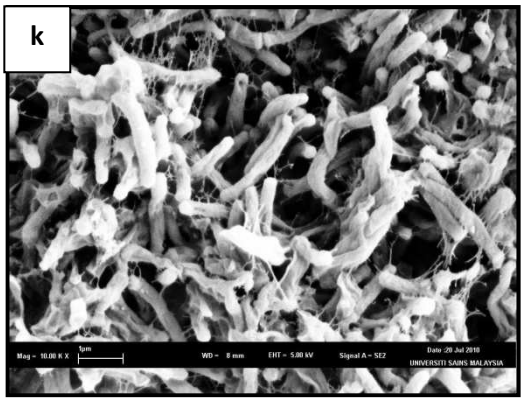

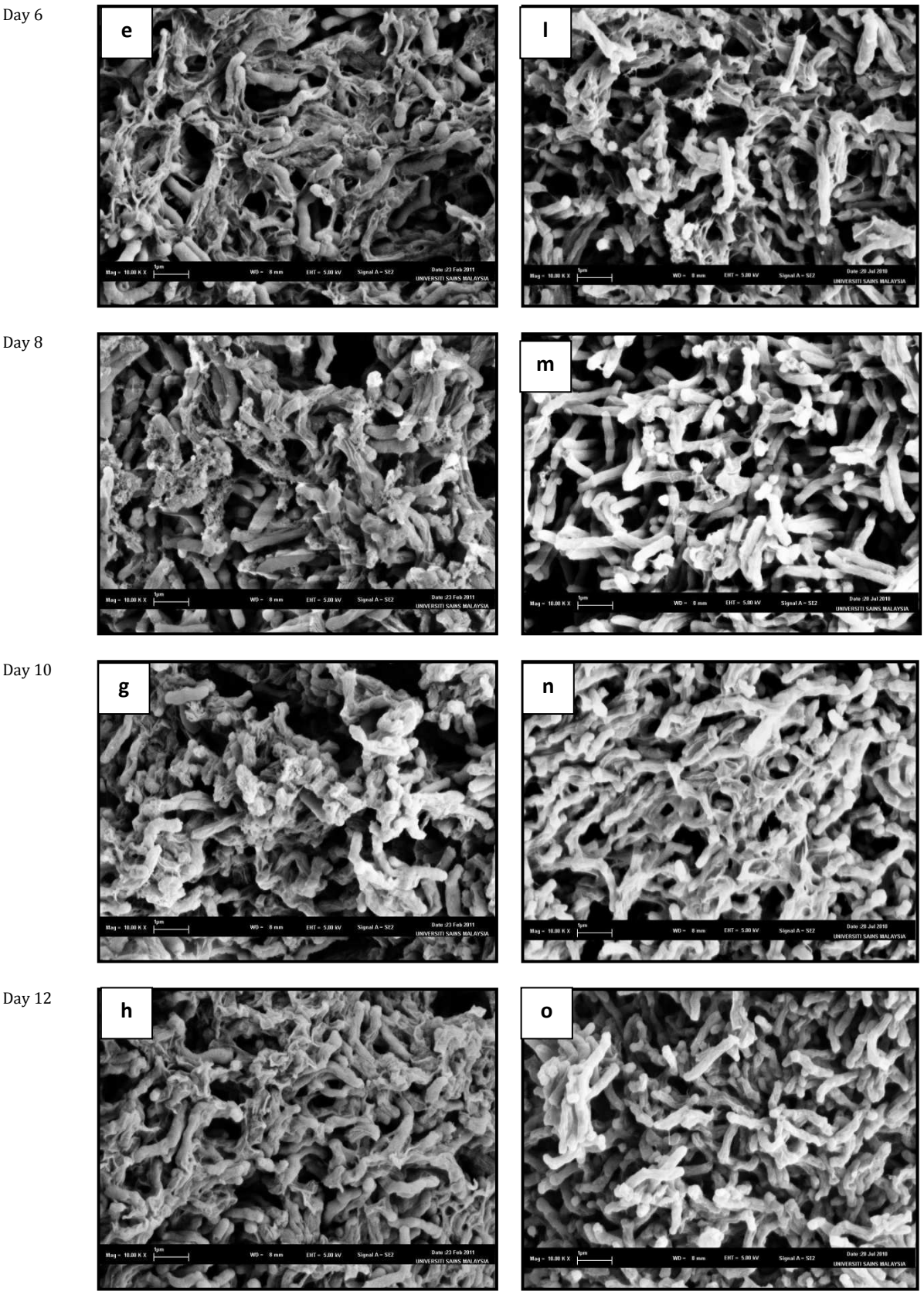

Fig. 4: Scanning electron micrographs. (a) Control, (b-h) isoniazid (INH), (i-o) 1-isonicotinoyl-2-hexadecanoyl hydrazine (INH-C16) treated cells.

The TEM observation revealed unequivocally striking differences in the cell wall morphology between the control, INH and INH-C16-treated cells. Figure 5 (a) shows the cells in the control culture on day 0. The cell envelope appeared well defined and rigid. The cell envelope was observed to have three layers as drawn schematically in Figure 5 (b).

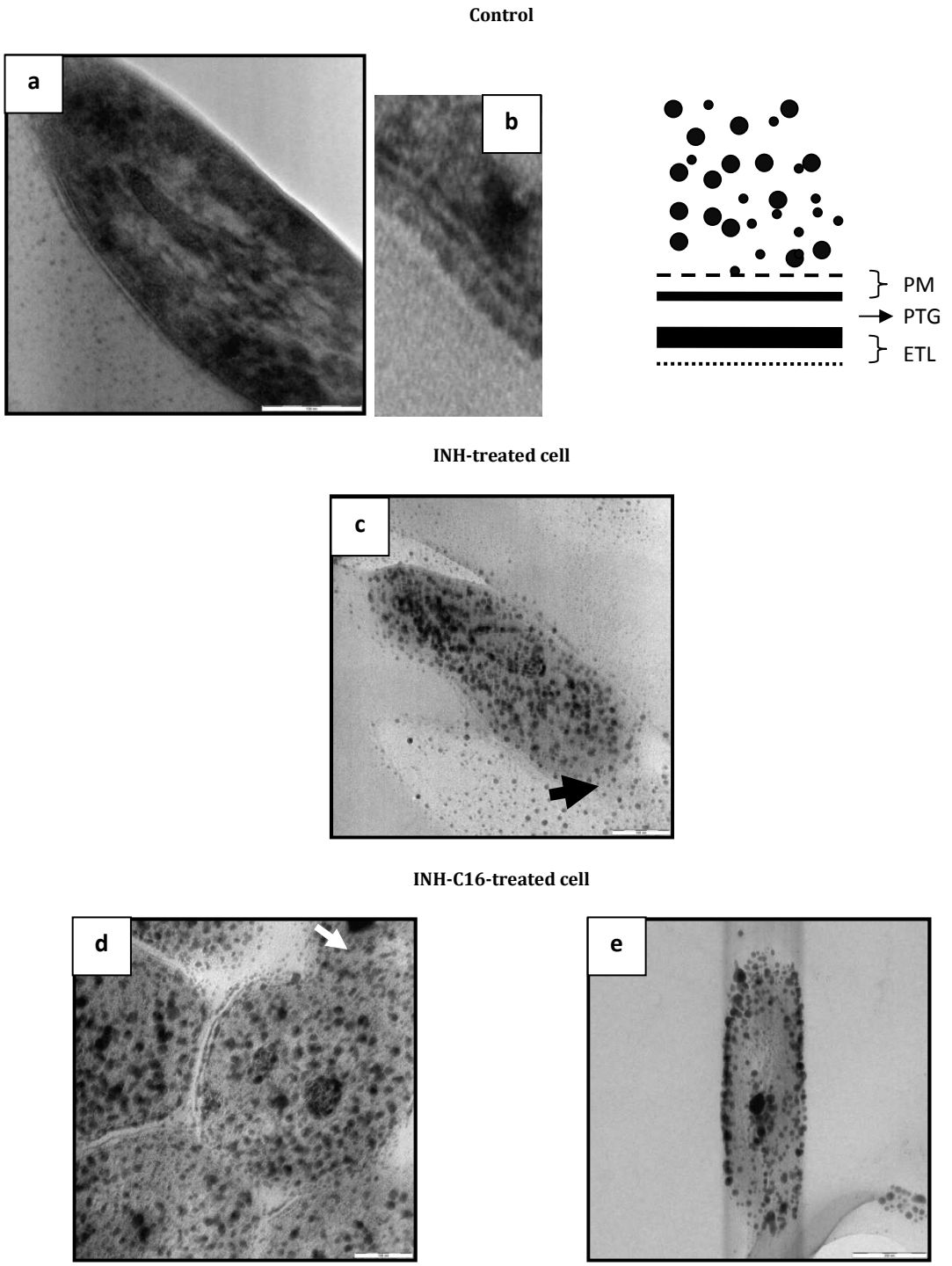

Fig. 5: Transmission electron micrographs. (a) Control, (b) schematic diagram of enlarged cell wall of control cell, (c) INH-treated cells, and (d-e) 1-isonicotinoyl-2-hexadecanoyl hydrazine-treated cells.

Figure 5 (c) shows the morphology of the INH-treated cells on day 4. This micrograph shows the fully lysed cell envelope with the extrusion of the intracellular contents (indicated by arrow). The ultrastructures of the INH-C16-treated cells on day 4 are shown in Figure 5 (d) and (e). Figure 5 (d) shows the collapsed mycobacterial cell wall which resulted in the extrusion of the cytoplasmic material from the ruptured point of the cell wall (indicated by arrow). Figure 5 (e) shows another observation that INH-C16 also caused the cell wall to lyse, similar to the INH-treated cell.

DISCUSSION

The MIC results obtained indicated that the addition of 16-carbon acyl carbon chain increased the degree of susceptibility *M. tuberculosis* H37Rv ATCC 25618 against INH by two-fold. The exposure of cells to INH and INH-C16 resulted in a significant reduction in the colony counts compared to the control. A similar growth pattern was observed in both the INH and INH-C16 treated culture, suggesting that INH-C16 exhibits similar strength of bactericidal activity as INH, even though at a lower concentration. These results indicated that the anti-TB activity of INH can be

enhanced by chemically augmenting the structure of INH with carbon side chain.

On the other hand, the INH and INH-C16 treated cells exhibited similar morphological and acid-fastness changes. However, marked differences in their effects on the *M. tuberculosis* H37Rv cells were not discernible under light microscopic observation. However, compared to the control cells, their effects on the cellular morphology of the mycobacteria were obvious. The effects can be summarized as follows. (i) The amorphous clumping of cells during the early days of treatment indicates immediate and rapid effects of the drugs. Like INH, the effects of INH-C16 had resulted rapid loss of cellular integrity which then caused the cells to form clumps. ii) The appearance of 'ghost' cells indicates that the cells were not able to retain the red basic fuchsin due to loss of acid-fastness characteristic. As fatty acids of the cell wall are the chemical basis for acid-fastness characteristic in *Mycobacterium* strains, therefore, loss of acid-fastness would be an indication that the cell envelope was damaged[21-24]

Observation under SEM showed that the control cells have a smooth surface, indicating that the cells were healthy at this stage. Besides, dividing cells were also observed during this period as indicated by the constrictions in between bacilli cells (Figure 4 (a), arrow A). This morphological characteristic suggests that the cells were about to multiply by binary fission as previously reported by Chatterjee et al.[25] and Dahl[26]. In addition, some cells were also observed to be connected parallel to each other over a large body part (Figure 4 (a), arrow B). Chatterjee et al.[25] suggested that this parallel arrangement might be due to the growth of daughter cell budding from the side of the mother cell and its subsequent growth along the side of the mother cell. Alternatively, the *M. tuberculosis* cells could go through a "snapping" post-fission movement during the cell division[26, 27]. In this growth process, the inner layer and plasma membrane would invaginate to form a new septum. Whereas, the outer layer remains intact until the splitting of the new septum upon the end of the septum formation, the inner layer may continuously grow and this exerts pressure on the outer layer. Eventually, this results in the splitting of the cell into two daughter cells that are connected side by side.

The INH and INH-C16-treated *M. tuberculosis* cells showed significant morphological changes compared to the control cells. Overall, the effects were found to be similar in both treatments. The key morphological changes observed in these treatments are summarized as follows. (i) The cells became wrinkled, ragged and clump to each other which give clear evidences of damages in the cell envelope. This also explains the formation of clumping cells in the light microscopic observation. (ii) The tiny holes observed on the cell surfaces indicate that INH and INH-C16 caused the cell wall to rupture. Similar observation was also reported by Takayama et al.[28] on *M. tuberculosis* H37Ra exposed to 0.5 µg/mL of INH. Hence, the findings of this study signify that cell wall rupture, which is a classical effect of INH, could also be of the effect of its derivative, INH-C16. (iii) The cell wall rupture resulted in the extrusion of cellular contents or cytoplasmic materials from the cells which could be the rationale for the "web-like" material formation around the cells. This visual observation could probably be due to the presence of either an alkali-extractable polysaccharide being released into the external medium by INH-treated cells as demonstrated in a study by Winder and Rooney[29], or protein materials as demonstrated in a later study by Bardou et al.[30]. Winder and Rooney[29] suggested that the mycolic acid inhibition in the cell wall by INH probably caused the intermediates of mycolic acid synthesis to be rechanneled into carbohydrate synthesis and some polysaccharides might also be extruded out through the damaged cell envelope. However, Bardou et al.[30] reported that the materials released from the INH-treated cells were mainly composed of proteins and the secretion of these proteins also decreased the mycolate content of the cell wall. They further explained that the inhibition of mycolic acid increases the permeability of the cell envelope and causes the cellular proteins to diffuse out of the cell. (iv) The extrusion of the cellular materials could have induced weaknesses in the cell envelope and eventually caused the cells to shrink. Finally, these damaged cells aggregated into an amorphous mass of cell debris.

TEM observation of the untreated control cell showed a typical cell envelope morphology of *M. tuberculosis* as reported by Takade et al.[31] and Velayati et al.[32]. The cell envelope was multi-layered consisting of: (1) an asymmetrical plasma membrane (PM) composed of a thicker outer and thinner inner leaflet, (2) a peptidoglycan (PTG) - an electron-dense layer associated with (PM) and (3) electron transparent layer (ETL) - an electron translucent layer outside the PTG layer.

The destruction of the cell wall of the INH and INH-C16-treated cells resulted in the extrusion of the cytoplasmic materials or the cell contents. Theoretically, this observation gives clear evidence of the "web-like" materials as observed under the SEM. The ruptured point in the cell wall seen in the INH-C16-treated cell adds windfall credit to the findings that INH-C16 could target the cell envelope which made it more permeable and hence, caused the cell content to burst out.

In an earlier study, Rastogi et al.[16] suggested that addition of lipophilic side chain to the parent INH compound increases the miscibility of INH in the lipid of mycobacterial cell envelope. Thus, this eases the penetration of the drug through the mycobacterial periplasmic space. In a subsequent similar study, Rastogi and Goh[14] proposed that palmitic acid chain in an amphipathic INH derivative could be metabolized which liberates the active INH molecules inside the bacteria. Hence, on the basis of these previous reports, it could be reckoned that the hydrophobic INH-C16 enters the mycobacterial cell by passive diffusion through the cell wall and is metabolized in such a way that would induce the active INH molecule to be liberated inside the bacteria. Ultimately, the active INH molecule causes disintegration of cell wall, which leads to cell death.

CONCLUSIONS

The findings of this study indicate that, increasing the hydrophobicity of INH by augmentation of hydrophobic side chain would positively improve the bactericidal activity of the drug. Microscopically, INH-C16 caused disorganization of the cell envelope that facilitated elution of some intracellular materials from the cells. It can be reckoned that the potential target of INH-C16 would be similar to INH which is via the inhibition of mycolic acid synthesis. Hence, INH-C16 is a potential effective anti-TB agent for further pharmacological investigation.

ACKNOWLEDGEMENTS

This research was supported by Fundamental Research Grant Scheme (FRGS) (203/PFARMASI/671157) and USM Fellowship Scheme. We express gratitude to the Veterinarian Research Institute, Bukit Tengah, Penang and the Electron Microscope Unit, School of Biological Sciences, USM for use of their microscopy facilities.

REFERENCE

1. Winder FG, Collins PB. Inhibition by isoniazid of synthesis of mycolic acids in *Mycobacterium tuberculosis*. J Gen Microbiol 1970; 63:41-8.
2. Takayama K, Wang L, David HL. Effect of isoniazid on the in vivo mycolic acid synthesis, cell growth, and viability of *Mycobacterium tuberculosis*. Antimicrob Agents Chemother 1972; 2:29-35.
3. Vilchèze C, Jacobs Jr WR. The mechanism of isoniazid killing: clarity through the scope of genetics. Annu Rev Microbiol 2007; 61:35-50.
4. Barkan D, Liu Z, Sacchettini JC, Glickman MS. Mycolic acid cyclopropanation is essential for viability, drug resistance, and cell wall integrity of *Mycobacterium tuberculosis*. Chem Biol 2009; 16:499-509.
5. WHO. Global tuberculosis control 2010. Accessed 17.01.2011: (http://whqlibdoc.who.int/publications/2010/9789241564069_eng.pdf.).
6. Kurniawati F, Sulaiman SAS, Gillani SW. Study on drug-resistant tuberculosis and tuberculosis treatment on patients with drug resistant tuberculosis in chest clinic outpatient department. IJPPS 2012; 4:733-7.

7. Vilchèze C, Morbidoni HR, Weisbrod TR, Iwamoto H, Kuo M, Sachettini JC, et al. Inactivation of the inhA-encoded fatty acid synthase II (FASII) enoyl-acyl carrier protein reductase induces accumulation of the FASI end products and cell lysis of *Mycobacterium smegmatis*. J Bacteriol 2000; 182:4059-67.
8. Ahmad S, Mustafa AS. Molecular diagnosis of drug-resistant tuberculosis. Kuw Med J 2001; 33:120-6.
9. Mendez JC. Multi drug resistance in tuberculosis and the use of PCR for defining molecular markers of resistance. Accessed 11/06/2011:(http://www.dcmsonline.org/jaxmedicine/2001journals/Feb2001/TBresistance.html).
10. Johnson R, Streicher EM, Louw GE, Warren RM, van Helden PD, Victor TC. Drug resistance in *Mycobacterium tuberculosis*. Curr Issues Mol Biol 2006; 8:97-112.
11. Somoskovi A, Parsons L, Salfinger M. The molecular basis of resistance to isoniazid, rifampin, and pyrazinamide in *Mycobacterium tuberculosis*. Respir Res 2001; 2:164-8.
12. Lee ASG, Teo ASM, Wong SY. Novel mutations in ndh in isoniazid-resistant *Mycobacterium tuberculosis* isolates. Antimicrob Agents Chemother 2001; 45:2157-9.
13. Rastogi N, Frehel C, David HL. Triple-layered structure of mycobacterial cell wall: evidence for the existence of a polysaccharide-rich outer layer in 18 mycobacterial species. Curr Microbiol 1986; 13:237-42.
14. Rastogi N, Goh KS. Action of 1-isonicotinyl-2-palmitoyl hydrazine against the *Mycobacterium avium* complex and enhancement of its activity by m-fluorophenylalanine. Antimicrob Agents Chemother 1990; 34:2061-4.
15. Rastogi N, Goh KS, David HL. Enhancement of drug susceptibility of *Mycobacterium avium* by inhibitors of cell envelope synthesis. Antimicrob Agents Chemother 1990; 34:759-64.
16. Rastogi N, Moreau B, Capmau ML, Goh KS, David HL. Antibacterial action of amphipathic derivatives of isoniazid against the *Mycobacterium avium* complex. Zentralbl Bakteriol Mikrobiol Hyg A 1988; 268:456-62.
17. Singh M, Raghav N. Biological activities of hydrazones: a review. IJPPS 2011; 3:26-32.
18. Besra GS, Minnikin DE, Wheeler PR, Ratledge C. Synthesis of methyl (Z)-tetracos-5-enoate and both enantiomers of ethyl (E)-6-methyltetracos-4-enoate: possible intermediates in the biosynthesis of mycolic acids in mycobacteria. Chem Phys Lipids 1993; 66:23-34.
19. Caviedes L, Delgado J, Gilman RH. Tetrazolium microplate assay as a rapid and inexpensive colorimetric method for determination of antibiotic susceptibility of *Mycobacterium tuberculosis*. J Clin Microbiol 2002; 40:1873-4.
20. Hoben HJ, Somasegaran P. Comparison of the pour, spread, and drop plate methods for enumeration of *Rhizobium* spp. in inoculants made from presterilized peat. Appl Environ Microbiol 1982; 44:1246-7.
21. Schaefer WB. Effect of isoniazid on the dehydrogenase activity of *Mycobacterium tuberculosis*. J Bacteriol 1960; 79:236-45.
22. Rastogi N, David HL. Mode of action of antituberculous drugs and mechanisms of drug resistance in *Mycobacterium tuberculosis*. Res Microbiol 1993; 144:133-43.
23. Barrera L. The basic of clinical bacteriology. In: Palomina JC, Leao SC, Ritacco V, eds. Tuberculosis 2007: from basic science to patient care: http://www.tuberculosistextbook.com /tuberculosis2007.pdf. 2007:93-112.
24. Yamada H, Bhatt A, Danev R, Fujiwara N, Maeda S, Mitarai S, et al. Non-acid-fastness in *Mycobacterium tuberculosis* ΔkasB mutant correlates with the cell envelope electron density. Tuberculosis 2012; 92:351-7.
25. Chatterjee KR, Gupta NND, De ML. Electron microscopic observations on the morphology of *Mycobacterium leprae*. Exp Cell Res 1959; 18:521-7.
26. Dahl JL. Electron microscopy analysis of *Mycobacterium tuberculosis* cell division. FEMS Microbiol Lett 2004; 240:15-20.
27. Thanky NR, Young DB, Robertson BD. Unusual features of the cell cycle in mycobacteria: polar-restricted growth and the snapping-model of cell division. Tuberculosis 2007; 87:231-6.
28. Takayama K, Wang L, Merkal RS. Scanning electron microscopy of the H37Ra strain of *Mycobacterium tuberculosis* exposed to isoniazid. Antimicrob Agents Chemother 1973; 4:62-5.
29. Winder FG, Rooney SA. The effects of isoniazid on the carbohydrates of *Mycobacterium tuberculosis* BCG. Biochem J 1970; 117:355-68.
30. Bardou F, Quemard A, Dupont M, Horn C, Marchal G, Daffe M. Effects of isoniazid on ultrastructure of *Mycobacterium aurum* and *Mycobacterium tuberculosis* and on production of secreted proteins. Antimicrob Agents Chemother 1996; 40:2459-67.
31. Takade A, Umeda A, Matsuoka M, Yoshida S, Nakamura M, Amako K. Comparative studies of the cell structures of *Mycobacterium leprae* and *M. tuberculosis* using the electron microscopy freeze-substitution technique. Microbiol Immunol 2003; 47:265-70.
32. Velayati AA, Farnia P, Ibrahim TA, Haroun RZ, Kuan HO, Ghanavi J, et al. Differences in cell wall thickness between resistant and nonresistant strains of *Mycobacterium tuberculosis*: using transmission electron microscopy. Chemotherapy 2009; 55:303-7.